Towards Autonomous Printable Robotics: Design and Prototyping of the Mechanical Logic

Wenzhong Yan (✉), Angela L. Gao, Yunchen Yu, and Ankur Mehta

The Laboratory for Embedded Machines and Ubiquitous Robots,

University of California, Los Angeles, CA 90095, USA

wzyan24@ucla.edu

Abstract—New strategies for controlling printable robots are needed for inexpensive and rapid integrated electromechanical prototyping. In this work, we propose a printable, easy-to-fabricate controller—what we refer to as the mechanical logic—which contains a bistable mechanism that acts as a mechanical switch which generates an oscillating binary electrical signal. The integration of the mechanical logic with conductive actuators endows it with clocking and current switching functions; thus, powered by a constant electrical energy source, the mechanical logic is able to autonomously control a sequence of actuations. To demonstrate this technique, we designed and fabricated prototypes of the mechanical logic, whose raw materials (not including the power supply) cost approximately 40 cents. Under a constant-current (0.55 A) power source, our mechanical logic was able to induce current oscillation with an average period of around 3.8 s. This property of the mechanical logic could ultimately be incorporated into onboard controllers for printable robots and devices.

Keywords: Printable robotics, Autonomous robots, Printable controllers, Design and prototyping

1. Introduction

The origami-inspired cut-and-fold technique allows for the application of 2D fabrication tools towards building 3D objects. Based on this technique, a new class of printable robots has been created. These printable robots are inexpensive, easy to design and manufacture, and amenable to rapid prototyping [1]. Therefore, they can be utilized for numerous real-life applications [2-5]. Nevertheless, in order to achieve autonomy, each printable robot still requires an on-board electrical controller, e.g. microcontroller, and its accessories, which raise the cost and the complexity of the resulting system. In this paper, therefore, we take a step towards inexpensive and easy electromechanical prototyping of robots: we present an inexpensive control method for fully printable robots, which allows for fast and inexpensive fabrication of a building block for robotics control. The mechanical logic, as shown in Fig. 1, has the potential to build an autonomous robot, once integrated with onboard power sources, printable structures and transducers.
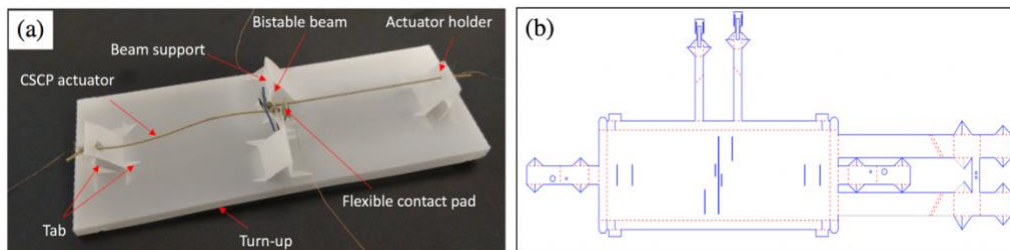

Fig. 1. (a) A prototype of the proposed mechanical logic (110 ✕ 40 ✕ 4 mm, 1.75g). Power is provided through tethers. (b) The corresponding 2D fold pattern of the origami structure. Blue lines represent cutting while red dash lines represent scoring. Actuators and other accessories are not shown here.

The presented approach allows for "printing" controlling methods for robots. The mechanical logic possesses clocking and current switching functions that are dictated by two factors, a switching mechanism and a time delay. The switching action is accomplished with

an origami precompressed bistable beam [6]. The deflection of this bistable beam enables it to store and release energy, giving rise to its two distinct stable positions. This characteristic makes it a great candidate for applications with two distinct working states, such as an on/off switch. Hence, bistable components can transform a continuous actuation into a sequence of discrete, transient motions. The time delay is realized with conductive supercoiled polymer (CSCP) actuators [7] that gradually contract in response to a steady Joule heating resulting from a constant power supply. The CSCP actuator is chosen for its special properties: high conductivity, low cost and easy fabrication.

Towards "printing" complete robotic systems, this paper focuses on a printable method for robots' controlling components. The contributions of this paper include:

- an electromechanical mechanism which generates an oscillating switched current from a constant electrical power supply;
- the low-cost design of a mechanical logic system which combines a bistable beam made with an origami-inspired strategy with CSCP actuators; and
- a printable control logic device featuring the proposed design, modeled, manufactured, and verified by experiments.

2. Related Work

Origami Origami was introduced to the robotics community in order to achieve easy, rapid and inexpensive robot prototyping. A wide variety of 3D geometries have been created out of origami structures by patterning 2D flat materials and assembling them by folding [8]. This technique has been applied to manufacturing varied printable robots. However, these printable robots still require custom or off-the-shelf, non-printable hardware, such as microcontrollers and electromechanical transducers, to achieve autonomy [9]. There has been an attempt to create printable elements to replace these electrical hardware [10], however, this work primarily focused on printing passive components and sensors, such as resistors and capacitors.

Controller Recently, Wehner et al. [11] developed an Octobot that incorporates a microfluidic logic [12] as an onboard controller to realize autonomy in fully soft robots. Similarly, Rothemund et al. [13] designed a soft, elastomeric valve that behaves as a mechanical "switch" which controls air flow for soft robots. When integrated into a feedback pneumatic circuit, the valve generates periodic motion using air from a single source of constant pressure, and acts as a pneumatic oscillator. Still, these works are not applicable to electromechanical robots, as they focused on entirely fluidic applications.

Inspired by these works, we came up with a printable controller that incorporates a bistable beam and CSCP actuators to achieve autonomy in origami-inspired, electrically powered printable robots, further reducing cost and increasing accessibility to the public.

3. Design and Modeling

3.1. Overall design and Mechanism

To implement the current-oscillating function, a bistable mechanism and conductive actuators are incorporated into an integrated design. Bistable mechanisms are ideal for switches because power is only needed for switching the beam between its stable states but not for maintaining it at one state. As shown in Fig. 2, the bistable mechanism functions as a double-pole, single-throw switch for both Loop A and Loop B in opposite phases. The actuators serve two functions: one of which is to complete the circuitry, while the other is to drive the snap-through motion of the bistable mechanism.

If the exerted force generated by the actuator exceeds the activation force required by the bistable mechanism, a snap-through motion of the bistable mechanism can be guaranteed. Under this circumstance, once power is supplied, the mechanical logic starts to oscillate: (1) initially, Loop A is closed. The corresponding actuator begins to heat up and gradually contract along its axial direction; (2) upon reaching its critical displacement, the bistable mechanism snaps to the other stable position; Loop A is now open while Loop B is closed; (3) Actuator A begins to cool down while Actuator B begins to heat up. The previous steps then execute for

the opposite loops; after this, the entire actuation process is completed. As the system repeats this entire process periodically, the mechanical logic behaves similarly to an electrical oscillator. The supplied power heats the actuators, and the thermal energy of these actuators subsequently dissipates into the atmosphere. Hence, to achieve continuous periodic oscillation, the time needed for the bistable mechanism to snap through must exceed the heat dissipation time of the actuators.
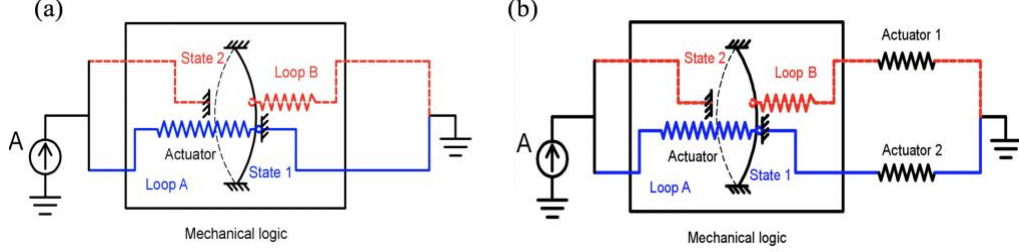

Fig. 2. A schematic of the mechanical logic and one of its possible applications. (a) The mechanism of the mechanical logic. Two loops are connected and disconnected alternatively when the bistable mechanism switches between the two different stable states, inducing current oscillation. (b) A possible configuration of a control-actuation system with the mechanical logic connecting with other actuators.

3.2. Function Implementation

1) CSCP actuator. In our system, the actuators are expected to implement the functions of both conductivity and actuation. CSCP actuators are chosen, since they are conductive and able to convert current into power and induce a temperature change, which can finally transform into their axial contraction. They are also low cost and easy to use.

The CSCP actuator is formed by twisting conductive polymer threads [14, 15] until they form coils and then annealing the coils thermally. The output force of the actuator can be described as follows [7]:

$$F = k(x - x_0) + b\dot{x} + c(T - T_0) \qquad (1)$$

where x and x_0 are the loaded and unloaded length of the actuator. k and b are the mean stiffness and mean damping coefficient of the actuator, respectively. T is the temperature of the actuator, while T_0 is the room temperature (i.e. 25°C), and c (a constant) is the mean slope to compensate the temperature rise of the actuator. For static or quasi-static analysis, the second (damping) term of Eq. (1) can be neglected.

The maximum strain of this kind of actuator is about 10% [14]. Under this limitation, the actuator's length (which results in the inverse change of k and b simultaneously) could alter the output force, which leads to the variation of the oscillation period of the mechanical logic. The power supply, which determines the temperature T, could also control the rate of change of the contraction force generated by the actuator, and therefore adjust the oscillation frequency of the mechanical logic. In conclusion, a longer CSCP actuator or higher power supply can increase the oscillation frequency of the mechanical logic.

2) Bistable beam switch. To design a mechanical logic capable of providing control for printable robots, we must come up with an easily fabricated mechanism with a switching function. In this work, a precompressed bistable beam is incorporated into the mechanical logic as a switch, since generating an axial load required for a precompressed beam with origami folding is relatively easy.

The beam is supported at its two terminals and subjected to a transverse force applied at its midpoint. Fig. 3 is a typical force-displacement diagram of a precompressed bistable beam, where state 1 and state 2 are its two distinct equilibrium states. The switching force, F_s, is the minimum force required for the bistable beam to switch from state 1 to state 2; the switch-back force, F_{sb}, is the minimum force required for the beam to switch back to state 1 from state 2. Both F_s and F_{sb} are referred to as critical forces, while the corresponding positions (u_s and u_{sb}) are critical displacements. u_{tr} refers to the distance its midpoint travels when the beam switches from one state to another. The snap-through occurs once the beam reaches its switching point, making it suitable as a switch, especially for our mechanical logic.
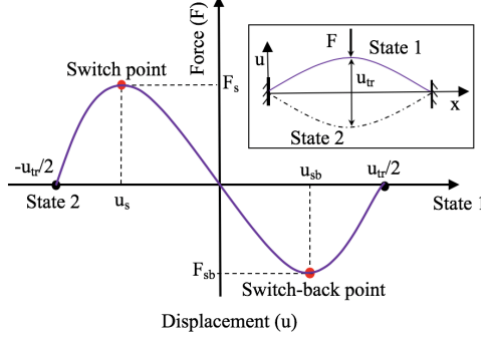
3

Fig. 3. A typical force-displacement curve of a precompressed bistable beam's middle point, adapted from [16].

The force-displacement curve of the bistable beam, which dictates its switching behavior, can be modeled using linear approximation. This curve is linearized around the beam's three equilibrium positions, and is thus composed of three linear curves [17].

$$F = \begin{cases} k_1(u + \dfrac{u_{tr}}{2}), & u \leq -u_0 \\[2mm] k_2 u, & -u_0 < u < u_0 \\[2mm] k_1(u - \dfrac{u_{tr}}{2}), & u \geq u_0 \end{cases}$$

$$k_1 = \frac{EI}{l^3}[\frac{10 - \pi^2}{16\pi^4} + \frac{EI}{d_0\pi^2 lEA - 4\pi^4 EI}]^{-1}$$

$$k_2 = -\frac{(2.86\pi)^2 EI}{l^3}[\frac{1}{4} - \frac{1}{2.86\pi}\tan(\frac{2.86\pi}{4})]^{-1} \tag{2}$$

$$u_0 = \frac{k_1 u_{tr}}{2(k_1 - k_2)}$$

where k_1 is the spring constant of the beam at its unstable equilibrium position, and k_2 is the spring constant at its two stable equilibrium positions. E, A, l, and I refer to the beam's Young's modulus, cross-section area, span, and moment of inertia, respectively. Moreover, d_0 is defined as the difference between the original length l_o and the span of the beam l.

The critical force and corresponding critical displacement are determined by the intersections of these linear curves, which, in turn, depend on the aforementioned parameters of the beam. Therefore, by carefully choosing the material (i.e. E) and the dimensional parameters of the bistable beam (i.e. A, I, l and l_0), we can control its behavior by predetermining its critical points (i.e. the critical force and the travel u_{tr}). Note that the actuation position on the bistable beam in our final design deviates slightly from its middle point; thus, the transverse force needed to facilitate the snap-through motion is expected to be smaller than the modeling result [18].

3.3. Mechanical Characterization

Since the mechanical logic is symmetrical, we only need to consider the actuation process on one side. To ensure a snap-through, the force generated by the actuator must exceed the activation force of the bistable beam. Mechanical testing is done using an Instron machine with an embedded heat chamber, which controls the temperature of actuators. To simulate the static behavior of the CSCP actuator, a simplified quasi-static model derived from Eq. (1) is established. Meanwhile, the force-displacement curve of the bistable beam is obtained from linear approximation [17].

For our characterization, a bistable beam with certain geometric parameters was chosen; we then explored the influence of the length of the CSCP actuator on its exerted force, in order to facilitate the mechanical logic design. The parameters of the beam and actuators are listed as follows: The length, width, thickness, and span of the beam are 14.9 mm, 3.0 mm, 0.1325 mm, and 14.0 mm, respectively. The Young's modulus of the beam is 3.0 GPa; k and c of the CSCP actuator (50 mm) are 186.8 ± 13.0 N · m and 28.6 ± 1.7 mN/°C. k of other actuators could be calculated, since it is inversely proportional to their lengths.

Modeling and experimental results are shown in Fig. 4. Fig. 4 (a) presents the forces generated by the actuators during contraction when their temperature reaches our predetermined working temperature. By changing the length of the actuator, we can tune the

attenuation of the output force against its contraction. As shown in the graph, the contraction force of a longer actuator tends to decrease much more slowly. With this theory, we are able to choose an actuator (of appropriate length) that can generate enough force to activate a bistable beam with certain geometry.
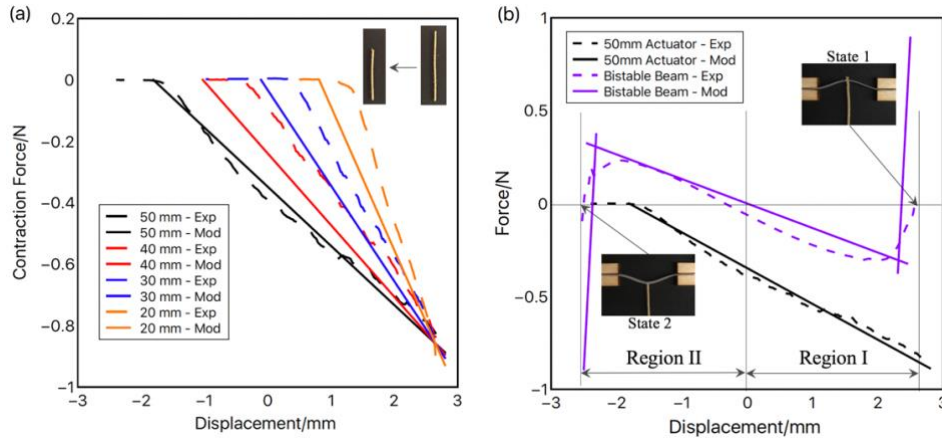

Fig. 4. Mechanical characterization of the mechanical logic, including modeling and experimental results. (a) Parametric study of the influence of the length of the CSCP actuator on its contraction force at 50°C. The range of the length investigated is between 20 and 50 mm, in 10 mm intervals. (b) The force-displacement curves of the chosen bistable beam and actuator (50mm). Activation is guaranteed when the contraction force generated by the actuator is greater than the beam's activation force in region I. In region II, the bistable beam can snap back if there is another actuator pulling on it in the opposite direction (not shown in the graph).

In our current work, we assume that the maximum working temperature of the actuator is 50°C (lower than its Glass Transition Temperature and melting point of the bistable beam). As shown in Region I of Fig. 4 (b), at 50°C, the force generated by the CSCP actuator is always greater than the activation force of the bistable beam, guaranteeing a snap-through motion. We do not need the force provided by this actuator to exceed the activation force of the beam in Region II of this graph, since in this region, the bistable beam is characterized by negative stiffness behavior. After the beam snaps through and quickly settles in its other equilibrium state, the actuator on the opposite side is expected to function in the same way, resulting in the snap-back motion of the beam.

Hence, we have demonstrated that the CSCP actuator can be integrated into the mechanical logic by showing that the force it generates exceeds the activation force of the bistable beam. Moreover, by varying the length of the actuator, we can control its output force (see Fig. 4) and thus the activation process of the bistable beam. Actuators with lengths from 40 mm to 50 mm can all trigger the bistable beam used in our experiment to snap through. These actuators of different lengths correspond to different activation times of the bistable beam, resulting in different oscillation periods of corresponding mechanical logics. Eventually, we chose 50 mm-long actuators for building our mechanical logic with the predetermined bistable beam, guaranteeing a highly fault-tolerant snap-through motion of the selected bistable beam. In other words, this actuator will be able to activate the bistable beam even if its working temperature deviates from the predetermined working temperature (50 °C).

4. Fabrication

4.1. Origami-inspired structure

The 2D planar design, shown in Fig. 1 (b), was accomplished in AutoCAD and cut using a Silhouette Cameo paper cutter to pattern a flat sheet. After cutting and folding, the final 3D model was created. There were several challenges in our origami-inspired structure fabrication, including the structure fastening, bistable beam formation, and flexible contact pads design.

1) Fastening method for the origami structure. To construct 3D structures out of 2D sheets, a fastening method was needed. To simplify fabrication and reduce cost, a mechanical tab was

created. This approach obviates the need for fasteners or adhesives during assembly. Two triangle ribs function together as a mechanical stopper to fix the position of the origami structure, as shown in Fig. 5 (Tab A). In some cases, folding the ribs to 90° against their attachment could force the structure itself to stand vertically against the base; in other words, this way of folding helps to shape the geometry of origami structures. Especially for the bistable beam formation, this approach not only helped to straighten the support of the beam, but also greatly increased the stiffness of the boundary of the beam (e.g. Tab B in Fig. 5). This enhanced stiffness is necessary for the symmetric operation of the bistable beam, as explained in the experiment section below.
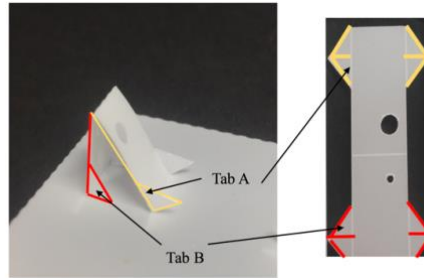

Fig. 5. A mechanical tab. Tab A is a typical mechanical tab, which can be used to fasten the structure. Tab B can help to keep the structure vertical against the base and increase its stiffness.

2) Bistable beam formation. In order to make the desired bistable beam out of a planar sheet, we needed to create a compliant beam with rigid supports which apply axial compression on it and result in buckling. This required that the flat sheet material itself should have flexibility. A low-cost .00'' polyester (PET) sheet was selected. We used a z-shape folding pattern and geometry confinement to form the precompressed bistable beam. The z-shape folding pattern (Fig. 6(a)) resulted in a first-step compression on the beam by decreasing its axial span. Then the beam fed through a slot in the support structure. The side walls of this slot could further confine the beam (Fig. 6(b)), giving rise to the final form of the desired bistable beam.
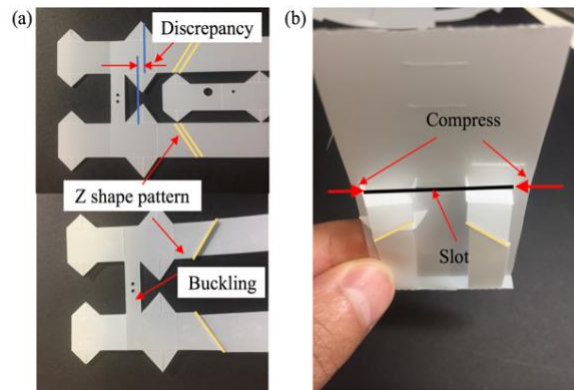

Fig. 6. A precompressed bistable beam formation. (a) z-shape folding is used to preliminarily compress the beam. Note that the discrepancy is exaggerated in the graph. (b) The axial dimension of the bistable beam is further confined by the sidewalls of the slot.

Due to the single-point confinement from each side wall, the bistable beam slightly bent upwards, with its symmetry broken. In order to keep the structure simple enough, we decided not to add accessories to balance the tilt. Instead, we compensated for the bending by differentiating the heights of the fastening tabs, as shown in Fig. 6(a). The discrepancy in the heights of tabs made the beam bend downwards, counteracting the initial error and therefore improving the symmetry of the bistable beam.

3) Contact pad design. In order to maintain the electrical connection in the loops before the bistable beam snaps through and realize an instant disconnection immediately thereafter, we designed a flexible contact pad, as shown in Fig. 7(a). The pad was made out of a

6

nonconductive PET sheet, and a piece of aluminum foil was attached on it to endow it with conductivity. As shown in Fig. 7(b), the critical displacement of the bistable beam is u_{cr}. If we settle the contact pad at the position $u = u_{cr} - \triangle$, its flexibility will ensure electrical connection between the actuator and contact pad before the bistable beam snaps through.
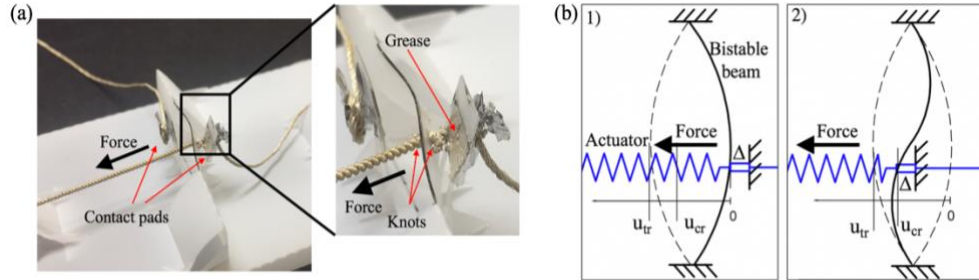

Fig. 7. A flexible contact pad. (a) The side view of the contact pad. (b) The arrangement of the bistable beam and the contact pad. 1) At the beginning, the flexible pad is at $u = -\triangle$. $\triangle$ is the length of the overhanging part of the actuator. 2) The actuator gradually pulls the beam leftwards and finally forces it to reach its critical displacement at $u = u_{cr}$. Meanwhile, the contact pad is at $u = u_{cr} - \triangle$.

4.2. Actuator fabrication and connectivity

Details of the CSCP actuators used in our paper can be found in [7]. Owing to the small contact area, the high contact resistance introduced on the connection between the actuator and the contact pad would lead to overheating. The overheating at the contact point would further increase its resistance or even melt the actuator, eventually destroying the conductivity of the circuit. In our work, we temporarily used conductive grease (Volume Electrical Resistivity 0.01 Ω-cm) to solve this problem. Before the experiment, a tiny volume of the conductive grease was spread on the terminal of actuator, shown in Fig. 7.

5. Experiments and Results

5.1. Testing Apparatus

The total cost of materials to build a mechanical logic with our approach is about 40 cents. After being fixed on the platform, the mechanical logic was powered with a constant current (0.55 A) by a laboratory power supply, as shown in Fig. 2. In addition, a cooling fan was added to control the period of oscillation by balancing the actuation rate and the heat dissipation rate of the actuator, as shown in Fig. 8.
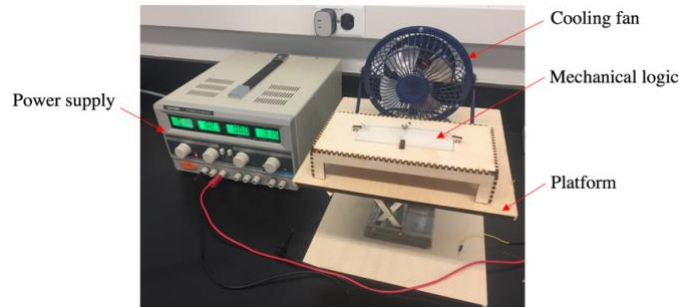

Fig. 8. The test rig for the mechanical logic. The position of the fan is fixed to maintain the same cooling condition of actuators for different tests.

5.2. Main Results

The test was run for around 20 seconds, during which the mechanical logic went through four complete oscillation cycles, along with one additional snap-through process at the very end. The result of the first cycle is represented in Fig. 9. At the very beginning, shown in Fig. 9(a), Loop A was connected, and then the corresponding Actuator A started to heat up. Once the contraction of Actuator A drove the bistable beam to its critical displacement (this

transition mode was noted at around 3.7 s, as indicated in Fig. 9(b)), the bistable beam snapped through and disconnected Loop A at about 3.8 s. At the same time, Loop B was connected. Then Actuator B heated up and contracted while Actuator A cooled down and relaxed. The system was back in a transition mode at around 5.8 s (see Fig. 9(d)), but oriented in the opposite direction. Thereupon, the bistable beam jumped back to its original position, completing the first oscillation at about 5.9 s. Thanks to the symmetrical design, the bistable beam continued this motion periodically, resulting in current oscillation.
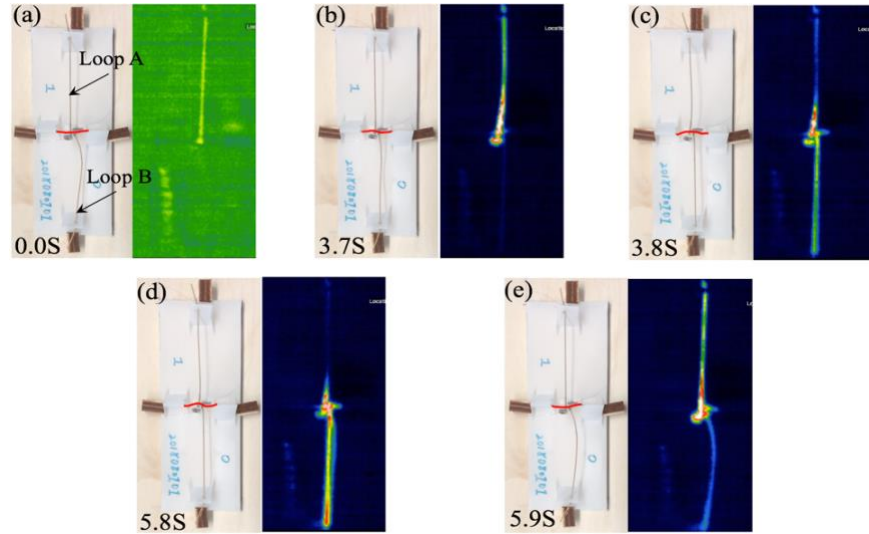

Fig. 9. The first oscillation cycle of the mechanical logic. For each figure from (a) to (e), the left part is the image of the mechanical logic and the right part is the corresponding thermal image from Seek Thermal Compact.

The average oscillation frequency (for four complete cycles) of this device was therefore about 0.27 Hz. This oscillation frequency is determined by the response time of the snap-through motion of the bistable beam. This response time depends on the bistable beam's dimension and the CSCP actuator's dynamic response, which, in turn, is determined by the input power and other parameters, according to the thermo-electro-mechanical model from [7].
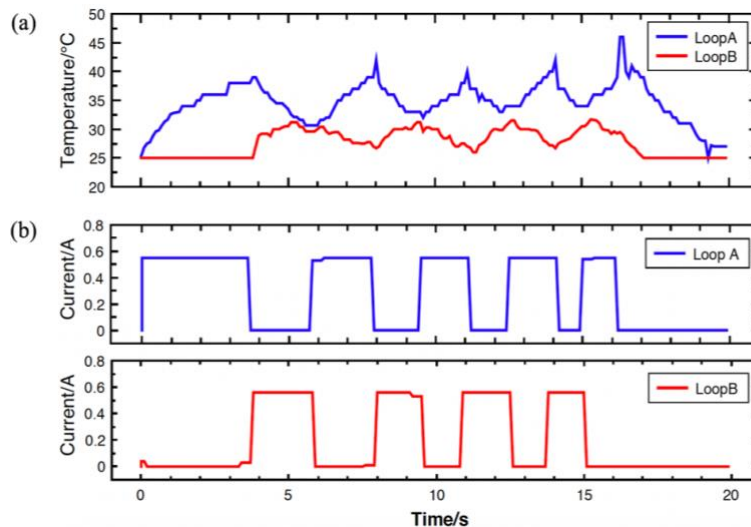

Fig. 10. Curves that show key variables (temperature and current) as a function of time. (a) Temperature curves of two actuators in both Loop A and Loop B. (b) Curves of currents through both Loop A and Loop B.

The currents running through both actuators, as well as these actuators' temperatures, are plotted in Fig. 10. The current graphs were created by plotting the readings from the multimeters over time, while the temperature changes were recorded with a thermal camera

(Seek Thermal Compact). In order to synchronize these two key variables (i.e. current and temperature) of the mechanical logic, we aligned two different curves by manually matching the critical moments when the current was first detected and when the temperature started to change. As shown in Fig. 10, two currents oscillated alternatively with an average period of about 3.75 s (the average of four complete cycles). Theoretically, decreasing the critical displacement of the bistable beam by changing its dimensions can allow it to snap through within a shorter time; thus, the oscillation frequency will increase correspondingly. In addition, the frequency of the current oscillation can be boosted by increasing the input power.

5.3. Discussion

1) Period Attenuation As shown in Fig. 10, the period of current oscillation decreased over time. This phenomenon could have resulted from the temperature rise of the CSCP actuators at the beginning of each cycle, which introduced a small initial contraction and further lessened the time needed to activate the snap-through of the bistable beam. Improving the stability of the CSCP actuators should eliminate this attenuation of the oscillation period. Still, this phenomenon implies a potential approach to tune the oscillation frequency by prestressing the actuators against the bistable beam. However, over-stressing of the actuators would destroy the bistability of the beam. Besides prestressing, changing the operating current, the length of the actuator, or the initial rise of the bistable beam could adjust the final characteristics of the oscillation, as mentioned above.

2) Thermal Asymmetry. The temperature curves of the two actuators are not symmetric, even though the structure of the system is. The different resistance at the two connections between the contact pads and the terminals of the actuators may account for this lack of symmetry. This hypothesis was verified by the thermal images (see Fig. 9) that each display a hot spot only at the connection between Actuator A and the corresponding contact pad. As the image shows in Fig. 10, Actuator A had higher maximum temperatures (around 41 °C) than Actuator B (about 33 °C) in all four cycles. Fortunately, this thermal asymmetry did not interfere with the functionality of the mechanical logic, though it altered the oscillation frequency. To resolve this issue of asymmetry, we plan to develop a more robust and controllable mechanism that connects the terminals of the actuators and the contact pads.

3) Oscillation Duration. The oscillation of the mechanical logic terminated after four complete cycles, while a longer oscillation duration is desired. The temperature of both actuators gradually fell back to room temperature; meanwhile, the current across both actuators dropped to zero. These phenomena might be explained by the disrupted conductivity at the connections between the actuators and the contact pads. In fact, a post-experiment examination of these connections verified this explanation: the connection between Actuator A and its corresponding contact pad was broken. Therefore, in order to obtain oscillations with longer duration, a better design of the connecting mechanism is needed.

6. Insights and Future Work

We demonstrated an entirely printable controller that, while using an external constant current power source, was able to generate periodic mechanical and electrical oscillations through the integration of a bistable beam and conductive actuators. The bistable beam acted as a switch, controlling electrical current flow through the actuators, which in turn drove the switching of the bistable beam. This resulting oscillation can be adapted for use in more complicated designs to sequence further switched actuators.

This was the first trial where an origami-inspired printable structure was incorporated into an autonomous printable controller for a robot. Thanks to the fabrication methods we adopted, the manufacturing of this controller was easy and inexpensive, leading to minimal cost of building a completely autonomous printable robot.

Our future work will include combining the mechanical logic with a printable robot body and additional actuators to create an integrated printable robot. The combination of the snap-through instability of a bistable beam with the contraction of CSCP actuators enables the mechanical logic to function on the component level, making it less sensitive to other

components of the robots (e.g., the actuators) and more predictable in its behavior. All of these advantages of the mechanical logic imply its easy integration into a printable robot. For example, we can use a worm-like robot [1] as a basic configuration, replace its NiTi coil actuators with conductive actuators (e.g. CSCP actuators), and add our mechanical logic as its controller, as shown in Fig. 1(b). With constant-current (or constant-voltage) power, the worm-like robot can undergo autonomous peristaltic locomotion.

To fabricate autonomous, untethered, and printable robots, the mechanical logic may also be combined with onboard energy sources (e.g. button battery). Furthermore, the printable energy sources (e.g. paper battery [19]) may ultimately be involved in designing a fully printable robot. We believe that our printable controller will be the foundation of manufacturing entirely printable, inexpensive, and autonomous robots, as well as a step towards making robots ubiquitous, accessible for every member of society.

References

[1] Onal, C.D., Wood, R.J., Rus, D.: An origami-inspired approach to worm robots. IEEE/ASME Transactions on Mechatronics 18 (2), 430–438 (2013).

[2] Mehta, A.M., Rus, D., Mohta, K., Mulgaonkar, Y., Piccoli, M., Kumar, V.: A Scripted Printable Quadrotor: Rapid Design and Fabrication of a Folded MAV, pp. 203–219. Springer International Publishing, Cham (2016).

[3] Martinez, R.V., Fish, C.R., Chen, X., Whitesides, G.M.: Elastomeric origami: Programmable paper elastomer composites as pneumatic actuators. Advanced Functional Materials 22(7), 1376–1384 (2012).

[4] Min, C.C., Suzuki, H.: Geometrical properties of paper spring. In: M. Mitsuishi, K. Ueda, F. Kimura (eds.) Manufacturing Systems and Technologies for the New Frontier, pp. 159–162. Springer London, London (2008)

[5] Kim, S.J., Lee, D.Y., Jung, G.P., Cho, K.J.: An origami-inspired, self-locking robotic arm that can be folded flat. Science Robotics 3 (16) (2018).

[6] Camescasse, B., Fernandes, A., Pouget, J.: Bistable buckled beam and force actuation: Experimental validations. International Journal of Solids and Structures 51(9), 1750–1757 (2014).

[7] Yip, M.C., Niemeyer, G.: On the control and properties of supercoiled polymer artificial muscles. IEEE Transactions on Robotics 33 (3), 689–699 (2017).

[8] Demaine, E.D., Demaine, M.L.: Recent results in computational origami. In: Origami 3: Proc. 3rd Int'l. Mtg. of Origami Science, Math, and Education (OSME2001), pp. 3–16. A K Peters, Monterey, California (2001)

[9] Mehta, A.M., DelPreto, J., Shaya, B., Rus, D.: Cogeneration of mechanical, electrical, and software designs for printable robots from structural specifications. In: Intelligent Robots and Syst. (IROS), pp. 2892–2897(2014).

[10] Miyashita, S., Meeker, L., Goldi, M., Kawahara, Y., Rus, D.: Self-folding printable elastic electric devices: Resistor, capacitor, and inductor. In: Conf. on Robotics and Automation (ICRA), pp. 1446–1453 (2014).

[11] Wehner, M., Truby, R.L., Fitzgerald, D.J., Mosadegh, B., Whitesides, G.M., Lewis, J.A., Wood, R.J.: An integrated design and fabrication strategy for entirely soft, autonomous robots. Nature 536, 451 (2016).

[12] Mosadegh, B., et al.: Integrated elastomeric components for autonomous regulation of sequential and oscillatory flow switching in microfluidic devices. Nature Physics 6(6), 433–437 (2010).

[13] Rothemund, P., Ainla, A., Belding, L., Preston, D.J., Kurihara, S., Suo, Z., Whitesides, G.M.: A soft, bistable valve for autonomous control of soft actuators. Science Robotics 3(16) (2018).

[14] Yip, M.C. and Niemeyer, G.: High-performance robotic muscles from conductive nylon sewing thread. In: Conf. on Robotics and Automation (ICRA), pp. 2313-2318 (2015).

[15] Zhang, D. and Rahmat-Samii, Y.: Integration of electro-textile RF coil array with magnetic resonance imaging (MRI) system: Design strategies and characterization methods. In 2018 International Workshop on Antenna Technology (iWAT), pp. 1-3 (2018).

[16] Palathingal, S. and Ananthasuresh, G.K.: Design of bistable pinned-pinned arches with torsion springs by determining critical points. In Mechanism and Machine Science, pp. 677-688 (2017).

[17] Vangbo, M.: An analytical analysis of a compressed bistable buckled beam. Sensors and Actuators A: Physical, 69(3), pp.212-216 (1998).

[18] Cazottes, P., Fernandes, A., Pouget, J. and Hafez, M.: Bistable buckled beam: modeling of actuating force and experimental validations. Journal of Mechanical Design, 131(10), p.101001 (2009).

[19] Hu, L, Choi, J.W., Yang, Y., Jeong, S., La Mantia, F., Cui, L.F., Cui, Y.: Highly conductive paper for energy-storage devices. Proceedings of the National Academy of Sciences 106 (51), 21,490–21,494 (2009).